Label-free enrichment of primary human skeletal progenitor cells using deterministic lateral displacement

Miguel Xavier [a,b], Stefan H. Holm [c], Jason P. Beech [c], Daniel Spencer [a], Jonas O. Tegenfeldt [c], Richard OC Oreffo [b] and Hywel Morgan [a]

[a] Faculty of Physical Sciences and Engineering, Institute for Life Sciences, University of Southampton, SO17 1BJ, United Kingdom.

[b] Centre for Human Development, Stem Cells and Regeneration, Institute of Developmental Sciences, Southampton General Hospital, Tremona Road, SO16 6YD Southampton, United Kingdom.

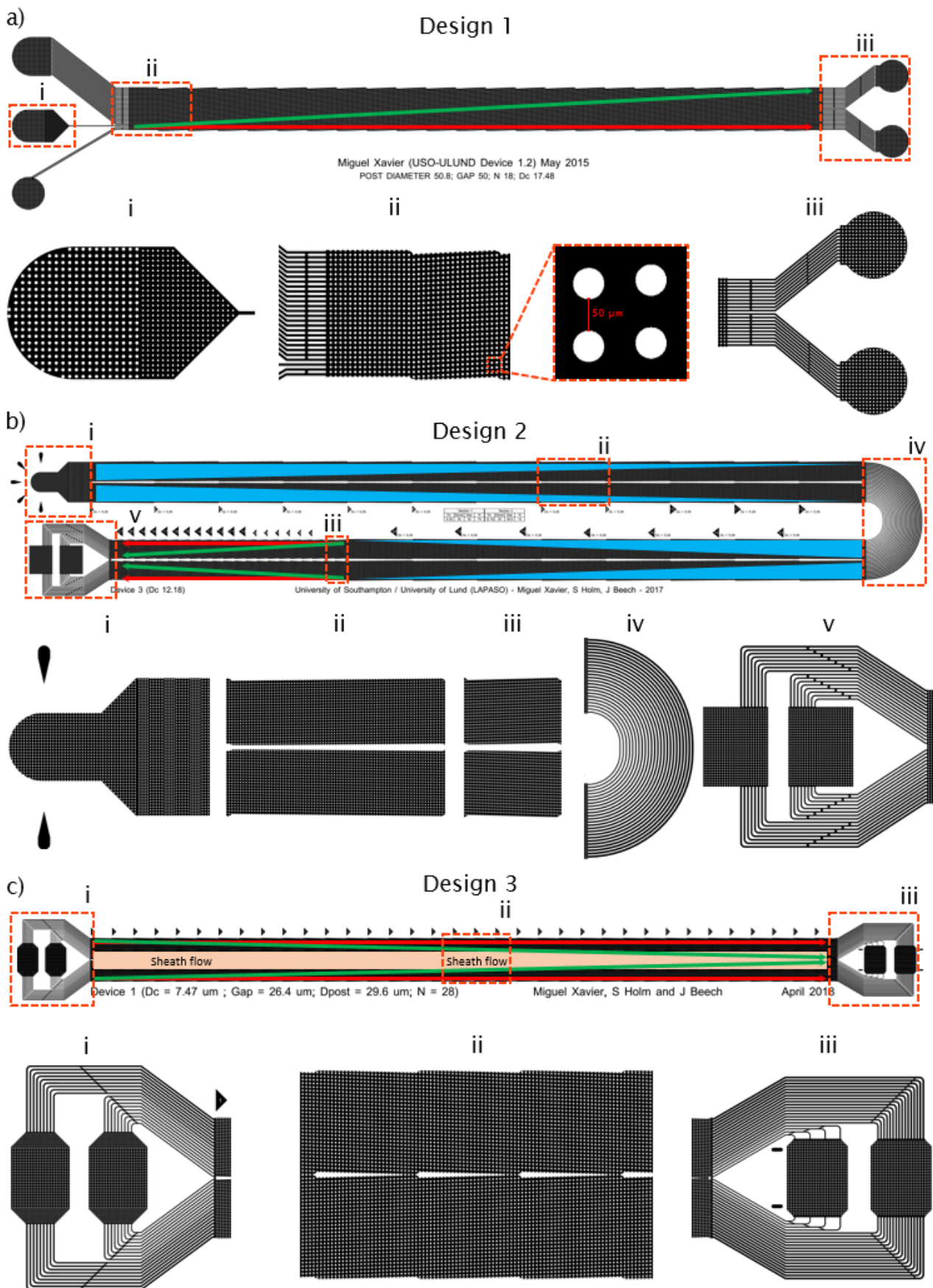[c] Division of Solid State Physics and NanoLund, Lund University, SE-221 00, Sweden

Electronic Supplementary Information

2. Materials & Methods

2.2 DLD design considerations

ESI Table 1 – Specifications of the mask designs of the deterministic lateral displacement devices. The device critical separation size (Dc = critical diameter) was calculated using the formula empirically derived by Davis[1] ($Dc = 1.4G \cdot N^{-0.48}$)

Device No.	Gap Size (G)	Post diameter (Dpost)	Period (N)	Migration Angle (θ)	Row Shift	Length (mm)	Width (mm)	Depth (μm)	Vertical Displacement (μm/mm)	Expected Critical Size (*Dc*)
1	50 μm	50.8 μm	18	3.18°	5.6 μm	41.1	2.7	50	55.6	17.48 μm
2 (section 1)	30 μm	30 μm	75	0.76°	0.8 μm	90.6	2.8	30	13.3	5.29 μm
2 (section 2)	30 μm	29.8 μm	13	4.40°	4.6 μm	17.0	2.8	30	76.9	12.18 μm
3	26.4 μm	29.6 μm	28	2.05°	2 μm	54.9	3.2	25	35.8	7.47 μm

ESI Figure 1 – Photolithography mask design close-ups. Magnifications of the mask drawings of DLD devices from designs 1 (a), 2 (b) and 3 (c) showing individual sections of key structures of the DLD devices used in this work. In a) - Device 1, note the unitary sample channel (i) that allows hydrodynamic focusing of the sample at the device entrance by adjacent sheath flow introduced at either side (ii). The sample:sheath ratio in device 1 was 1:25, which led to significant sample dilution and reduced throughput. In b) – Device 2, note the use of a mirrored micropillar array (ii) that allows creating a central cell-free stream when using a sheathless device to increase throughput. In c) – Device 3, note the combination of sheath flow (i) and a mirrored micropillar array (ii) to achieve sorting with high resolution and low sample dilution (sample:sheath, 1:1).

Xavier *et al.* 2018 Label-free enrichment of primary human bone marrow progenitor cells using deterministic lateral displacement – Electronic Supplementary Information

2.3. Device design and fabrication

Edge correction

A parabolic flow profile occurs between the micropost arrays in DLD and is key for efficient particle separation. However, this profile holds only for infinitely wide arrays and becomes perturbed at the interface between the array and the sidewall flow significantly degrading sorting efficiency. To minimise this effect, Inglis[2] proposed a method for edge correction that assures that $1/N^{th}$ of the total fluid will flow over each post at all times, with N the period of the array. The solution was to adjust the gap size between the pillar rows closest to the walls of the device. The gap between each post and the wall of the zigzagging and the bumping sides is given by Equations 1 and 2 respectively, where n is the column number in a displacement array assuming values from 1 to N, G the gap size and ψ the tangent of the particle migration angle. An example of edge correction calculations in shown in ESI Table 2.

$$G_{zigzag}(n) = G\sqrt{n\psi} \quad (Equation\ 1)$$

$$G_{bumping}(n) = G\sqrt{2 - n\psi} \quad (Equation\ 2)$$

**ESI Table 2 –** Example of edge correction calculations for design 1.

1	2	3	4	5	6	7	8	9	10	11	12	13	14	15	16	17	18	N
11.79	16.67	20.41	23.57	26.35	28.87	31.18	33.33	35.36	37.27	39.09	40.82	42.49	44.10	45.64	47.14	48.59	50.00	Gap before zigzag wall
69.72	68.72	67.70	66.67	65.62	64.55	63.46	62.36	61.24	60.09	58.93	57.74	56.52	55.28	54.01	52.70	51.37	50.00	Gap before bumping wall

Hydraulic resistance calculations

Whenever different sections of the DLD devices were connected by rectangular channels with varying lengths, the channel width was adjusted accordingly to guarantee an identical hydraulic resistance across the device span, which was estimated for each channel using equation 3,[3] where w, h and L are the channel dimensions and η the fluid viscosity. Computational fluid dynamics simulations in COMSOL Multiphysics 4.3 (COMSOL AB, Stockholm, Sweden) were conducted to verify that both flow and particle profiles were preserved (ESI Figure 2 a-c). These steps were crucial to assure that particles maintained their relative positions before and after the connecting sections channels.

$$R = \frac{12\eta L}{wh^3}\left[1 - \frac{h}{w}\left(\frac{192}{\pi^5}\sum_{n=1}^{\infty}\frac{1}{(2n-1)^5}tanh\left(\frac{(2n-1)\pi w}{2h}\right)\right)\right]^{-1} \quad (Equation\ 3)$$
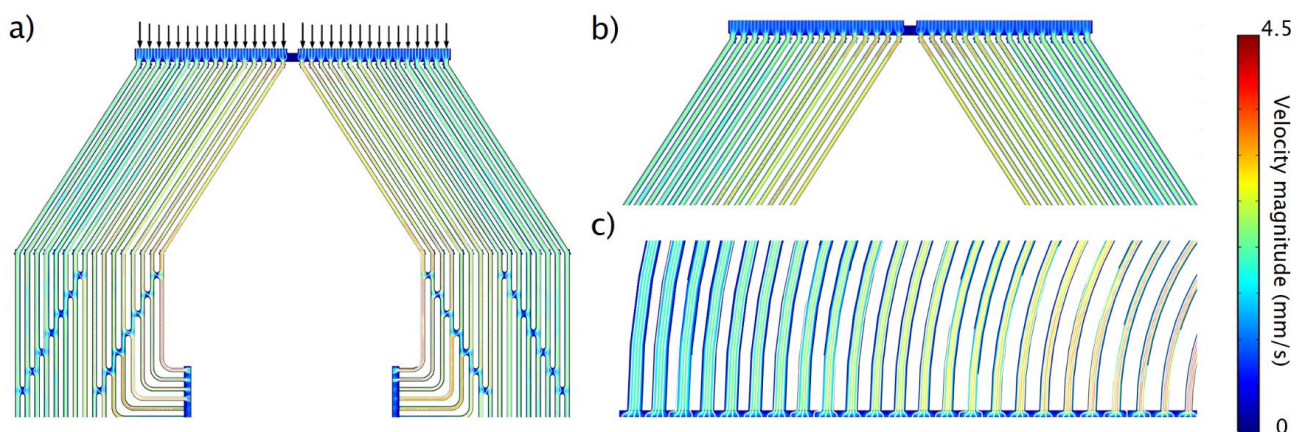
ESI Figure 2 – Computational fluid dynamics simulation. 2-D plots of critical sections (a and b, channel outlets; and c, curved connecting channels) from design 2 devices with channels of different length and width. Streamlines demonstrate that the flow is split evenly before entering each channel. This ensures that particles will retain their relative lateral position between sections. The 2-D simulations were conducted using COMSOL Multiphysics 4.3.

Detailed microfabrication methods

Briefly, wafers were cleaned in fuming nitric acid, dehydrated overnight at 210 ℃ and spin-coated (3,000 rpm, 30 s) with TI Prime to promote adhesion of the photo-resist. An SU-8 formulation was chosen according to the projected feature height, spin-coated for 30 s and soft baked before UV exposure using an EVG® 620T mask aligner (EV Group, St. Florian am Inn, Austria). Wafers were finally post-exposure baked, developed in EC solvent and hard baked. The feature height was verified using a KLA-Tencor surface profiler (CA, USA). Details of the process specifications are listed in ESI, Table 3. The silicon master moulds were pre-treated with a layer of hydrophobic 1H,1H,2H,2H-per-fluorooctyl-trichlorosilane to facilitate de-moulding. Sylgard® 184 PDMS elastomer was prepared by mixing the elastomer with curing agent (10:1, w/w), degassed and cured over the mould at 80 ℃ for one hour. Inlets/outlets were opened using a 1.5 mm biopsy punch (Kai Europe GmbH, Solingen, Germany). The PDMS stamps were oxygen plasma bonded to PDMS-coated glass-slides using a Femto Plasma Asher (Diener electronic GmbH + Co. KG, Germany).

ESI Table 3 – Microfabrication specifications for the silicon master moulds of devices 1-3.

Feature height	25 µm (device 3)	30 µm (device 2)	50 µm (device 1)
SU-8	SU-8 3025	SU-8 3025	SU-8 50
Spin-coating speed	3,000 rpm	2,500 rpm	2,000 rpm
Pre-exposure bake	65 ℃, 2 minutes	65 ℃, 2 minutes	65 ℃, for 6 minutes
	95 ℃, 11 minutes	95 ℃, 12 minutes	95 ℃, for 20 minutes
Exposure dose	165 mJ·cm^{-2}	180 mJ·cm^{-2}	200 mJ·cm^{-2}
Post-exposure bake	65 ℃, 1 min.	65 ℃, 1 minute	65 ℃, for 1 minute
	95 ℃, 3 minutes 20 seconds	95 ℃ 3 minutes 40 seconds	95 ℃, for 5 minutes
Development	5 minutes 30 secs.	6 minutes	6 minutes
Hard bake	150 ℃, for 20 minutes	150 ℃, for 20 minutes	150 ℃, for 20 minutes

2.5 Device operation
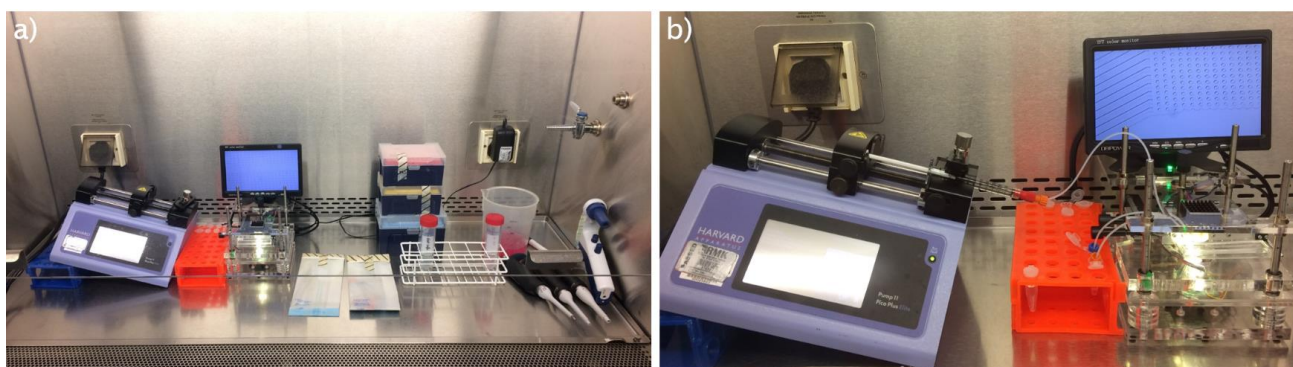
ESI Figure 3 – DLD device operation in a sterile environment (laminar flow hood). A portable microscope built in-house was used to monitor the flow stability.

2.6. Cell Culture

Cells were maintained in media supplemented with 10 % foetal calf serum (FCS) and 100 U·mL^{-1} penicillin and 100 µg·mL^{-1} streptomycin (1 % Pen/Strep). This is referred to as complete media. Otherwise, it is indicated as plain media. Cells were maintained in a humidified chamber at 37 ℃ and 5 % CO_2.

MG-63

MG-63 human osteosarcoma cells (passages 27 to 30) were obtained from the European Collection of Authenticated Cell Cultures (ECACC, UK) and cultured in complete DMEM. The culture media was replenished every 2-3 days and the cells were routinely sub-cultured assuring a maximum confluence of 70% and re-plated at a cell seeding density of 2-4 x 10^4 cells·cm^{-2}.

GFP$^+$ MG-63

GFP$^+$ MG-63 cells were established in previous work by transduction with a retroviral pMX-GFP vector (Cell Biolabs Inc., VPK-302)[4] containing a green fluorescent protein (GFP) insert and using polybrene as a transduction enhancer.[4] Culture of GFP$^+$ MG-63 cells was under the same conditions as non-transfected MG-63.

HL-60

HL-60, human peripheral blood promyelocytic leukaemia cells were obtained from the European Collection of Authenticated Cell Cultures (ECACC, UK) and cultured in complete RPMI-1640 media. The cells were split every other day to a concentration of 2×10^5 cells·mL^{-1}.

2.8. Flow cytometry

HL-60 labelling with CellTracker™ Deep Red Dye

HL-60 were washed in PBS, suspended in 1 µM CellTracker™ deep red dye (C34565 from Invitrogen™) in pre-warmed plain RPMI and incubated for 45 minutes in a humidified chamber at 37 ℃ and 5 % CO$_2$. After incubation, the dye was removed by centrifugation and the cells washed twice with PBS before analysis.

Skeletal stem cell labelling with CellTracker™ Green CMFDA Dye

Adhered SSCs were washed with PBS, pre-treated with collagenase IV (200 µg·mL^{-1}) in plain α-MEM for 40 to 60 min. and incubated with 10 µM CellTracker™ green CMFDA (C7025 from Invitrogen™) in pre-warmed plain α-MEM for 45 minutes. After incubation, the dye was removed and the cells were further cultured in complete α-MEM for 60 minutes to encourage the conversion of the chloromethyl group into cell-impermeable products by cytosolic esterases. Cells were then washed with PBS and lifted as detailed above.

White blood cell labelling of CD45

WBCs from whole blood were fluorescently labelled for CD45 by incubation with an APC-conjugated anti-human CD45 antibody (Miltenyi Biotec 130-098-143) for 20 minutes under agitation, in the dark. RBC lysis was performed as in the main text.

2.9. Statistical Analyses

ESI Table 4 – Standard normal distribution. Table values (negative) represent area to the left of the Z-score.

Z	0	0.01	0.02	0.03	0.04	0.05	0.06	0.07	0.08	0.09
-4.0	0.00003	0.00003	0.00003	0.00003	0.00003	0.00003	0.00002	0.00002	0.00002	0.00002
-3.9	0.00005	0.00005	0.00005	0.00005	0.00006	0.00006	0.00006	0.00006	0.00007	0.00007
-3.8	0.00007	0.00008	0.00008	0.00008	0.00008	0.00009	0.00009	0.00010	0.00010	0.00010
-3.7	0.00011	0.00010	0.00010	0.00010	0.00009	0.00009	0.00008	0.00008	0.00008	0.00008
-3.6	0.00016	0.00015	0.00015	0.00014	0.00014	0.00013	0.00013	0.00012	0.00012	0.00011
-3.5	0.00023	0.00022	0.00022	0.00021	0.00020	0.00019	0.00019	0.00018	0.00017	0.00017
-3.4	0.00034	0.00032	0.00031	0.00030	0.00029	0.00028	0.00027	0.00026	0.00025	0.00024
-3.3	0.00048	0.00047	0.00045	0.00043	0.00042	0.00040	0.00039	0.00038	0.00036	0.00035
-3.2	0.00069	0.00066	0.00064	0.00062	0.00060	0.00058	0.00056	0.00054	0.00052	0.00050
-3.1	0.00097	0.00094	0.00090	0.00087	0.00084	0.00082	0.00079	0.00076	0.00074	0.00071
-3.0	0.00135	0.00131	0.00126	0.00122	0.00118	0.00114	0.00111	0.00107	0.00104	0.00100
-2.9	0.00187	0.00181	0.00175	0.00169	0.00164	0.00159	0.00154	0.00149	0.00144	0.00139
-2.8	0.00256	0.00248	0.00240	0.00233	0.00226	0.00219	0.00212	0.00205	0.00199	0.00193
-2.7	0.00347	0.00336	0.00326	0.00317	0.00307	0.00298	0.00289	0.00280	0.00272	0.00264
-2.6	0.00466	0.00453	0.00440	0.00427	0.00415	0.00402	0.00391	0.00379	0.00368	0.00357
-2.5	0.00621	0.00604	0.00587	0.00570	0.00554	0.00539	0.00523	0.00508	0.00494	0.00480
-2.4	0.00820	0.00798	0.00776	0.00755	0.00734	0.00714	0.00695	0.00676	0.00657	0.00639
-2.3	0.01072	0.01044	0.01017	0.00990	0.00964	0.00939	0.00914	0.00889	0.00866	0.00842
-2.2	0.01390	0.01355	0.01321	0.01287	0.01255	0.01222	0.01191	0.01160	0.01130	0.01101
-2.1	0.01786	0.01743	0.01700	0.01659	0.01618	0.01578	0.01539	0.01500	0.01463	0.01426
-2.0	0.02275	0.02222	0.02169	0.02118	0.02068	0.02018	0.01970	0.01923	0.01876	0.01831
-1.9	0.02872	0.02807	0.02743	0.02680	0.02619	0.02559	0.02500	0.02442	0.02385	0.02330
-1.8	0.03593	0.03515	0.03438	0.03362	0.03288	0.03216	0.03144	0.03074	0.03005	0.02938
-1.7	0.04457	0.04363	0.04272	0.04182	0.04093	0.04006	0.03920	0.03836	0.03754	0.03673
-1.6	0.05480	0.05370	0.05262	0.05155	0.05050	0.04947	0.04846	0.04746	0.04648	0.04551
-1.5	0.06681	0.06552	0.06426	0.06301	0.06178	0.06057	0.05938	0.05821	0.05705	0.05592
-1.4	0.08076	0.07927	0.07780	0.07636	0.07493	0.07353	0.07215	0.07078	0.06944	0.06811
-1.3	0.09680	0.09510	0.09342	0.09176	0.09012	0.08851	0.08691	0.08534	0.08379	0.08226
-1.2	0.11507	0.11314	0.11123	0.10935	0.10749	0.10565	0.10383	0.10204	0.10027	0.09853
-1.1	0.13567	0.13350	0.13136	0.12924	0.12714	0.12507	0.12302	0.12100	0.11900	0.11702
-1.0	0.15866	0.15625	0.15386	0.15151	0.14917	0.14686	0.14457	0.14231	0.14007	0.13786
-0.9	0.18406	0.18141	0.17879	0.17619	0.17361	0.17106	0.16853	0.16602	0.16354	0.16109
-0.8	0.21186	0.20897	0.20611	0.20327	0.20045	0.19766	0.19489	0.19215	0.18943	0.18673
-0.7	0.24196	0.23885	0.23576	0.23270	0.22965	0.22663	0.22363	0.22065	0.21770	0.21476
-0.6	0.27425	0.27093	0.26763	0.26435	0.26109	0.25785	0.25463	0.25143	0.24825	0.24510
-0.5	0.30854	0.30503	0.30153	0.29806	0.29460	0.29116	0.28774	0.28434	0.28096	0.27760
-0.4	0.34458	0.34090	0.33724	0.33360	0.32997	0.32636	0.32276	0.31918	0.31561	0.31207
-0.3	0.38209	0.37828	0.37448	0.37070	0.36693	0.36317	0.35942	0.35569	0.35197	0.34827
-0.2	0.42074	0.41683	0.41294	0.40905	0.40517	0.40129	0.39743	0.39358	0.38974	0.38591
-0.1	0.46017	0.45620	0.45224	0.44828	0.44433	0.44038	0.43644	0.43251	0.42858	0.42465
0.0	0.50000	0.49601	0.49202	0.48803	0.48405	0.48006	0.47608	0.47210	0.46812	0.46414

ESI Table 5 – Standard normal distribution. Table values (positive) represent area to the left of the Z-score.

| Z	0	0.01	0.02	0.03	0.04	0.05	0.06	0.07	0.08	0.09
0	0.50000	0.50399	0.50798	0.51197	0.51595	0.51994	0.52392	0.52790	0.53188	0.53586
0.1	0.53983	0.54380	0.54776	0.55172	0.55567	0.55962	0.56356	0.56749	0.57142	0.57535
0.2	0.57926	0.58317	0.58706	0.59095	0.59483	0.59871	0.60257	0.60642	0.61026	0.61409
0.3	0.61791	0.62172	0.62552	0.62930	0.63307	0.63683	0.64058	0.64431	0.64803	0.65173
0.4	0.65542	0.65910	0.66276	0.66640	0.67003	0.67364	0.67724	0.68082	0.68439	0.68793
0.5	0.69146	0.69497	0.69847	0.70194	0.70540	0.70884	0.71226	0.71566	0.71904	0.72240
0.6	0.72575	0.72907	0.73237	0.73565	0.73891	0.74215	0.74537	0.74857	0.75175	0.75490
0.7	0.75804	0.76115	0.76424	0.76730	0.77035	0.77337	0.77637	0.77935	0.78230	0.78524
0.8	0.78814	0.79103	0.79389	0.79673	0.79955	0.80234	0.80511	0.80785	0.81057	0.81327
0.9	0.81594	0.81859	0.82121	0.82381	0.82639	0.82894	0.83147	0.83398	0.83646	0.83891
1	0.84134	0.84375	0.84614	0.84849	0.85083	0.85314	0.85543	0.85769	0.85993	0.86214
1.1	0.86433	0.86650	0.86864	0.87076	0.87286	0.87493	0.87698	0.87900	0.88100	0.88298
1.2	0.88493	0.88686	0.88877	0.89065	0.89251	0.89435	0.89617	0.89796	0.89973	0.90147
1.3	0.90320	0.90490	0.90658	0.90824	0.90988	0.91149	0.91309	0.91466	0.91621	0.91774
1.4	0.91924	0.92073	0.92220	0.92364	0.92507	0.92647	0.92785	0.92922	0.93056	0.93189
1.5	0.93319	0.93448	0.93574	0.93699	0.93822	0.93943	0.94062	0.94179	0.94295	0.94408
1.6	0.94520	0.94630	0.94738	0.94845	0.94950	0.95053	0.95154	0.95254	0.95352	0.95449
1.7	0.95543	0.95637	0.95728	0.95818	0.95907	0.95994	0.96080	0.96164	0.96246	0.96327
1.8	0.96407	0.96485	0.96562	0.96638	0.96712	0.96784	0.96856	0.96926	0.96995	0.97062
1.9	0.97128	0.97193	0.97257	0.97320	0.97381	0.97441	0.97500	0.97558	0.97615	0.97670
2	0.97725	0.97778	0.97831	0.97882	0.97932	0.97982	0.98030	0.98077	0.98124	0.98169
2.1	0.98214	0.98257	0.98300	0.98341	0.98382	0.98422	0.98461	0.98500	0.98537	0.98574
2.2	0.98610	0.98645	0.98679	0.98713	0.98745	0.98778	0.98809	0.98840	0.98870	0.98899
2.3	0.98928	0.98956	0.98983	0.99010	0.99036	0.99061	0.99086	0.99111	0.99134	0.99158
2.4	0.99180	0.99202	0.99224	0.99245	0.99266	0.99286	0.99305	0.99324	0.99343	0.99361
2.5	0.99379	0.99396	0.99413	0.99430	0.99446	0.99461	0.99477	0.99492	0.99506	0.99520
2.6	0.99534	0.99547	0.99560	0.99573	0.99585	0.99598	0.99609	0.99621	0.99632	0.99643
2.7	0.99653	0.99664	0.99674	0.99683	0.99693	0.99702	0.99711	0.99720	0.99728	0.99736
2.8	0.99744	0.99752	0.99760	0.99767	0.99774	0.99781	0.99788	0.99795	0.99801	0.99807
2.9	0.99813	0.99819	0.99825	0.99831	0.99836	0.99841	0.99846	0.99851	0.99856	0.99861
3	0.99865	0.99869	0.99874	0.99878	0.99882	0.99886	0.99889	0.99893	0.99896	0.99900
3.1	0.99903	0.99906	0.99910	0.99913	0.99916	0.99918	0.99921	0.99924	0.99926	0.99929
3.2	0.99931	0.99934	0.99936	0.99938	0.99940	0.99942	0.99944	0.99946	0.99948	0.99950
3.3	0.99952	0.99953	0.99955	0.99957	0.99958	0.99960	0.99961	0.99962	0.99964	0.99965
3.4	0.99966	0.99968	0.99969	0.99970	0.99971	0.99972	0.99973	0.99974	0.99975	0.99976
3.5	0.99977	0.99978	0.99978	0.99979	0.99980	0.99981	0.99981	0.99982	0.99983	0.99983
3.6	0.99984	0.99985	0.99985	0.99986	0.99986	0.99987	0.99987	0.99988	0.99988	0.99989
3.7	0.99989	0.99990	0.99990	0.99990	0.99991	0.99991	0.99992	0.99992	0.99992	0.99992
3.8	0.99993	0.99993	0.99993	0.99994	0.99994	0.99994	0.99994	0.99995	0.99995	0.99995
3.9	0.99995	0.99995	0.99996	0.99996	0.99996	0.99996	0.99996	0.99996	0.99997	0.99997
4	0.99997	0.99997	0.99997	0.99997	0.99997	0.99997	0.99998	0.99998	0.99998	0.99998

2.10 Materials

BioWhittaker® Dulbecco's modified Eagle medium with glucose and L-glutamine (DMEM), alpha minimum essential medium with deoxyribonucleotides, ribonucleotides and ultra-glutamine (α-MEM), RPMI-1640, Dulbecco's phosphate buffered saline (PBS), foetal calf serum (FCS) and trypsin/EDTA with glucose were obtained from Lonza (Basel, Switzerland). Penicillin-streptomycin 100x, AB human serum, collagenase IV, ethylenediamine tetra-acetic acid (EDTA), crystal violet, Ficoll® PM400, Trichloro(1H,1H,2H,2H-perfluorooctyl)silane and Pluronic® F-127 were purchased from Sigma-Aldrich (St. Louis, MO, USA). Non-deformable polystyrene beads for size-based sorting were from Polysciences Europe GmbH (Germany). Bovine serum albumin (BSA) was obtained from GE Healthcare (Chicago, IL, USA). Lymphoprep™ was bought from Stem Cell Technologies (Vancouver, Canada). Anti-mouse IgM microbeads, LS MACS™ columns and the QuadroMACS™ separator were purchased from Miltenyi Biotec (Bergisch Gladbach, Germany). TI Prime, SU-8 50 and SU-8 3025 were from Microchem Corp. (Westborough, MA, USA). The EC solvent was from Dow® Microposit® (MicroResist Technology GmbH, Germany). S-Monovette® 9NC tri-sodium citrate tubes were obtained from Sarstedt (Nümbrecht, Germany) and Sylgard® 184 polydimethylsiloxane (PDMS) was purchased from VWR (Darmstadt, Germany). All reagents were used as received and according to the manufacturer's recommendations.

Results and discussion

3.2. Device 2

#### 3.2.1. Size and Mechano-based sorting of MG-63 and HL-60
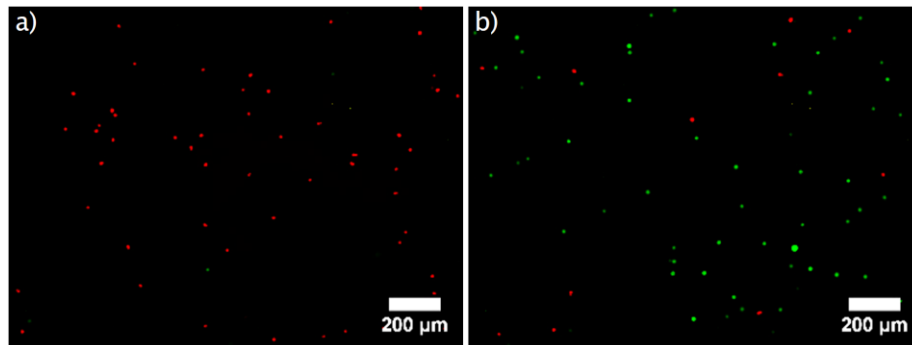
ESI Figure 4 – Fluorescence microscopy images (Zeiss Axiovert 200 microscope, 5x objective) of the cell fractions sorted at a flow rate of 15 µL·min^{1} and collected at the smaller-cell (a) and larger-cell (b) outlets respectively. To facilitate cell discrimination, GFP^{+} MG-63 were used together with CellTracker™ (deep red) labelled HL-60 cells.

#### 3.2.2. Binary fractionation of SSCs as a function of cell deformability
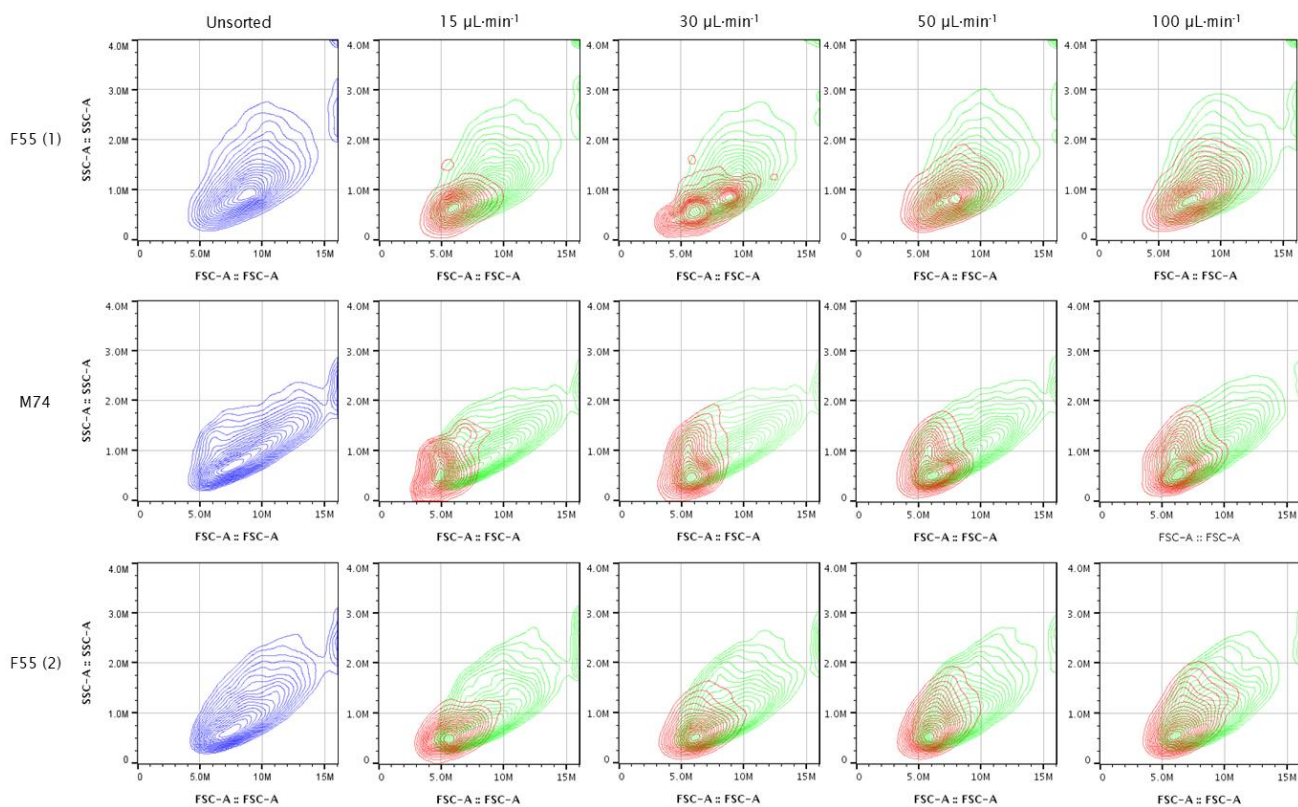
ESI Figure 5 – Forward (FSC-A) and side (SSC-A) scatter distributions of expanded human skeletal stem cells, unsorted (blue) and collected at the smaller-cell (red) and larger-cell (green) outlets after fractionation by DLD. Contour levels were set at 5 %.
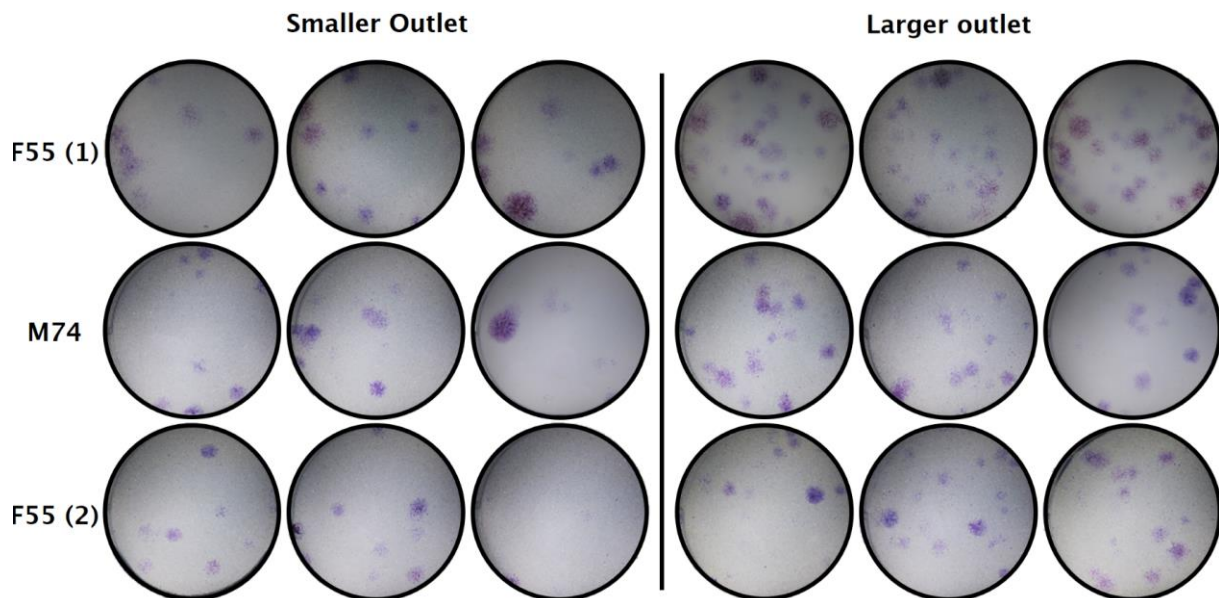
ESI Figure 6 – Colony forming units-fibroblastic (CFU-F), counterstained with crystal violet, growing in wells of a 6-well plate. Expanded human skeletal stem cells were sorted by DLD at 15 μL·min^{-1}, collected from the smaller-cell and larger-cell outlets and plated at a cell seeding density of 10 cells·cm^{-2}. Cells collected at the larger-cell outlet appear to display a higher capacity to form clonogenic cultures.
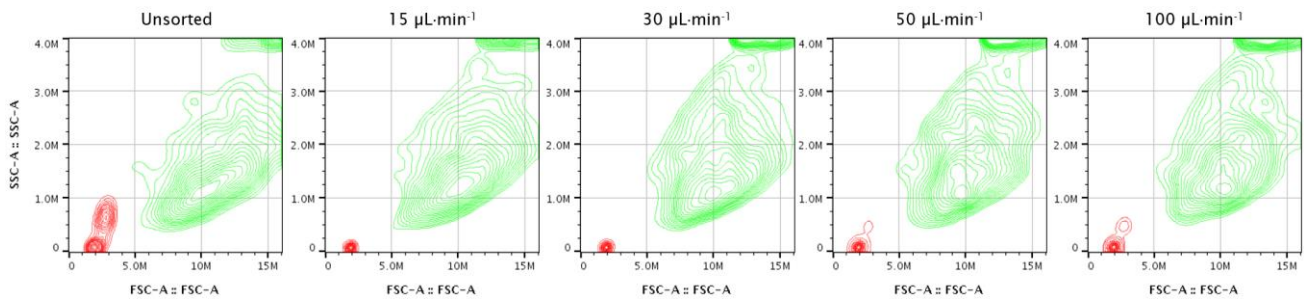
ESI Figure 7 – Forward (FSC-A) and side (SSC-A) scatter distributions of CD45-labelled WBCs (red) and SSCs (green) labelled with CellTracker™ green, unsorted and collected at the larger-cell outlet after label-free sorting by DLD. Contour levels were set at 5 %. Interestingly, at 15 µL·min^{-1} it was the smallest fraction of WBCs (possibly lymphocytes) that appeared in the larger-cell outlet. With increasing flow rate, the size distribution spread to gradually include larger cells but still excluded the largest WBCs. This led to the conclusion that cell deformation resulted in the smallest WBC sub-populations changing their effective size to diameters below the D_C of section 1 (5.3 µm). This effect was exacerbated at highest flow rates, when cell deformation became more significant.

3.3. Device 3

3.3.1. Enrichment of primary human bone marrow mononuclear cells
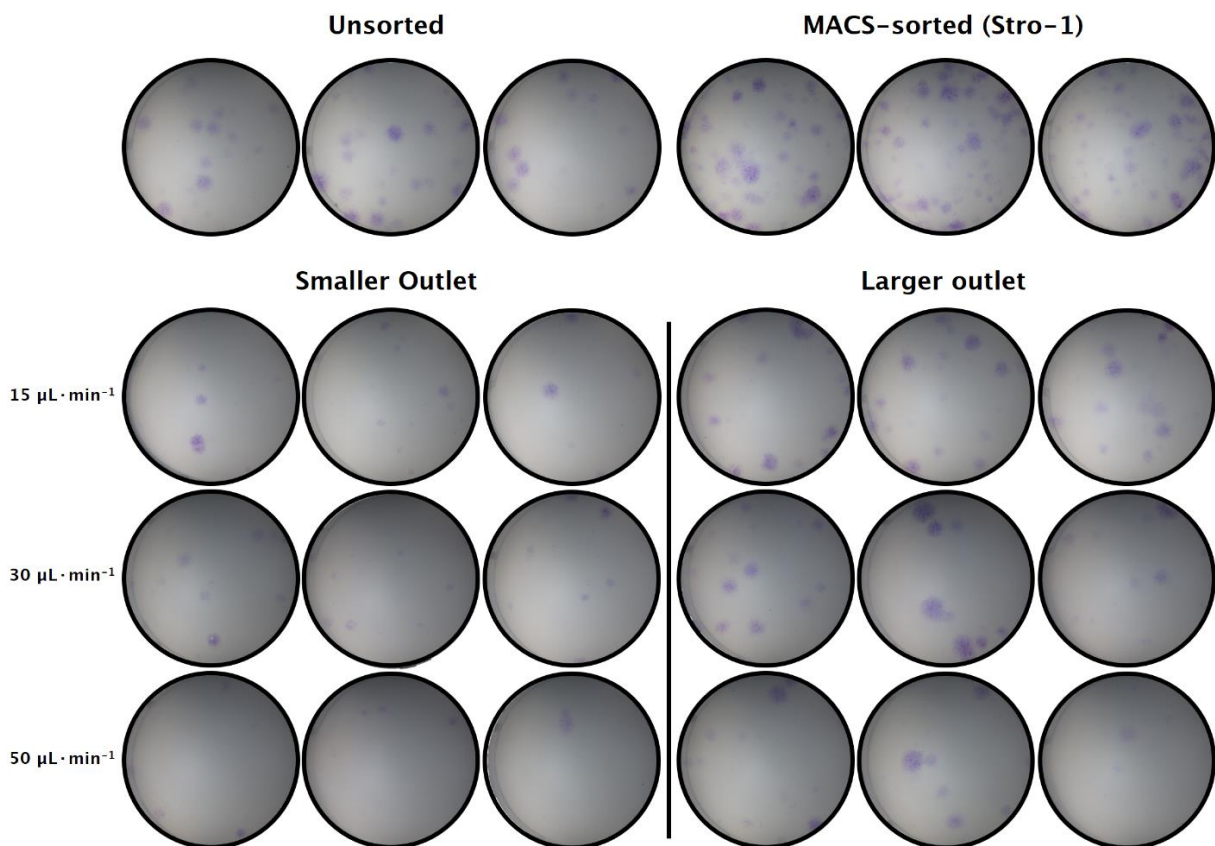
ESI Figure 8 – Colony forming units-fibroblastic (CFU-F), counterstained with crystal violet, growing in wells of a 6-well plate. Human bone marrow mononuclear cells were sorted by DLD at , collected from the smaller-cell and larger-cell outlets and plated at a cell seeding density of 10,000 cells·cm^{-2}. Cells collected at the larger-cell outlet appear to display a higher capacity to form clonogenic cultures.

References

1. Davis, J. A. Microfluidic Separation of Blood Components through Deterministic Lateral Displacement. (Princeton University, 2008).
2. Inglis, D. W. Efficient microfluidic particle separation arrays. *Appl. Phys. Lett.* **94,** 013510 (2009).
3. Bruus, H. *Theoretical microfluidics*. (Oxford University Press, 2008).
4. Czekańska, E. M. In vitro cell and culture models for osteoblasts and their progenitors. (Cardiff University, 2014).